Functional interaction of tumor suppressor DLC1 and caveolin-1 in cancer cells

Xiaoli Du[1], **Xiaolan Qian**[1], **Alex Papageorge**[1], **Aaron J. Schetter**[2], **William C. Vass**[1], **Xi Liu**[1], **Richard Braverman**[1], **Ana I. Robles**[2], and **Douglas R. Lowy**[1]

[1]Laboratory of Cellular Oncology, Center for Cancer Research, National Cancer Institute, National Institutes of Health, Bethesda, MD 20892, USA

[2]Laboratory of Human Carcinogenesis, Center for Cancer Research, National Cancer Institute, National Institutes of Health, Bethesda, MD 20892, USA

Abstract

Deleted in liver cancer 1 (DLC1), a tumor suppressor gene frequently inactivated in non-small cell lung cancer (NSCLC) and other malignancies, encodes a multidomain protein with a RhoGTPase-activating (RhoGAP) domain and a StAR-related lipid transfer (START) domain. However, no interacting macromolecule has been mapped to the DLC1 START domain. Caveolin-1 (CAV1) functions as a tumor suppressor in most contexts and forms a complex with DLC1. Here, we have mapped the region of DLC1 required for interaction with CAV1 to the DLC1 START domain. Mutation of the DLC1 START domain disrupted the interaction and co-localization with CAV1. Moreover, DLC1 with a START domain mutation failed to suppress neoplastic growth, although it negatively regulated active Rho. CAV1 and DLC1 expression levels were correlated in two public datasets of NSCLC lines and in two independent publicly available mRNA expression datasets of NSCLC tumors. Clinically, low DLC1 expression predicted a poor clinical outcome in patients with lung cancer. Together, our findings indicate that complex formation between the DLC1 START domain and CAV1 contributes to DLC1 tumor suppression via a RhoGAP-independent mechanism, and suggest that DLC1 inactivation probably contributes to cancer progression.

Keywords

DLC1; CAV1; StART; tumor suppressor gene; RhoGAP

Introduction

The tumor suppressor gene deleted in liver cancer 1 (DLC1) is frequently down-regulated in several malignancies, including lung, colorectal, breast, prostate, and liver cancer (1-3). DLC1 proteins are composed of three recognized domains: a Sterile alpha motif (SAM) domain, a Rho GTPase activating protein (RhoGAP) domain, and a StAR-related lipid

Corresponding author: Douglas R. Lowy, Laboratory of Cellular Oncology, Building 37, Room 4106, Center for Cancer Research, National Cancer Institute, National Institutes of Health, Bethesda, MD 20892, USA; Phone: 301-496-9513; Fax: 301-480-5322; lowyd@mail.nih.gov.

No potential conflicts of interest were disclosed.

transfer (START) domain. The SAM domain of DLC1 has been reported to interact with Eukaryotic elongation factor 1A1 (EF1A1), which facilitates the distribution of EF1A1 to the membrane periphery and to ruffles upon growth factor stimulation (4). The RhoGAP domain contributes to the tumor suppressor function for DLC1 by accelerating the conversion of active Rho-GTP to inactive Rho-GDP, which stimulates remodeling of the cytoskeleton as well as inhibiting neoplastic growth and cell migration (5-7). Other START domains are reported to mediate lipid sensing, lipid binding, and lipid exchange (8, 9), but no functional interaction has been linked to the DLC1 START domain.

To better understand the tumor suppressor function of DLC1 beyond its RhoGAP activity, it has been useful to explore the interactions between DLC1 and other proteins, and their biological consequences. Previous studies have shown that DLC1 interacts, in a physiologically relevant manner, with several proteins, such as members of the tensin focal adhesion protein family, FAK, and talin (10-14), which bind sequences located between the SAM and RhoGAP domains. DLC1 interacts with other proteins, including p120RasGAP and S100A10 (15, 16).

Caveolin 1 (CAV1) is the principal structural component and marker of caveolae. It was first indentified as a tyrosine-phosphorylated substrate when avian fibroblasts were transformed with the v-Src oncogene (17). CAV1 is reported to affect tumor progression, including growth, metastasis, and angiogenesis. In most instances, it functions as a tumor suppressor, although in others, it may positively regulate tumorigenesis (18). Here, focusing on DLC1 and CAV1 in NSCLC, we have mapped an interaction between DLC1 and CAV1 to the DLC1 START domain and shown the interaction is necessary for the tumor suppressing activity of DLC1. In addition, analysis of publicly available expression profiling microRNA array data indicated that the expression of DLC1 and CAV1 are positively correlated, and that the level of DLC1 expression is an independent prognostic factor in lung cancer patients.

Materials and Methods

Plasmid constructs

The GFP-tagged full length DLC1 (GFP-DLC1, the R718A GAP-dead mutant [GFP-DLC1(R718A), and the fragments encoding DLC1 residues 1-492 and 500-1091 (GFP-DLC1(1-492) and GFP-DLC1(500-1091), respectively), in the pEGFP-N1 vector (Clontech Laboratories, Palo Alto, CA), have been previously described (47). The truncated cDNA fragments encoding DLC1 residues 500-798, 500-638 and 623-1091 were subcloned in frame into pEGFP-N1. The deletions of DLC1 aa 899-996, 899-928, 929-957, and 957-996 were introduced into full-length GFP-DLC1 cDNA with a site-directed mutagenesis kit (Strategene, La Jolla, CA). Using the same kit, deletion of amino acids 617-624 was introduced into GFP-DLC1(500-1091). Human full length CAV1 (Source BioScience LifeSciences, Nottingham, UK) was cloned in to the eukaryotic pEBG expression vector (48). All constructs were verified by DNA sequencing.

Cell culture and Transfection

A549, H1703, H157, H727 (American Type culture Collections, Manassas, VA) and H358, H1299 (from Dr. Curt Harris, National Cancer Institute, Bethesda) were cultured in RPM1640 supplemented with 10% fetal bovine serum (FBS). HEK293T (49) cells were maintained in DMEM supplemented with 10% FBS. Cells were cultured at 37°C in a humidified 5% CO2 atmosphere. Cells were transfected using Lipofectamine 2000 (Invitrogen, Carlsbad, CA) according to the manufacturer's instructions. Stable clones expressing GFP, GFP-DLC1-WT and GFP-DLC1-Del(929-957) were obtained by transfection of H358 cells with Lipofectamine 2000 followed by selection with G418 (0.8 μg/ml).

siRNA Transfection

Control siRNA and validated siRNAs for human DLC1 (siRNA-5 and -11) were from Qiagen (Qiagen, Valencia, CA). The target sequences are 5′-GCCGATGTCGTAATTCCTATA-3′ and 5′-CTGGAGTGTAGGAATTGACTA-3′ for DLC1. Human CAV1 SMART pool siRNA was from Dharmacon (Dharmacon RNAi Technologies, Lafayette, CO). Cells were transfected with siRNAs as indicated for 24 hours using lipofectamine 2000, followed by a change of media. For migration assays, cells were trypsinized and collected after an additional 48 hours.

Immunofluorescent Staining and Microscopy

Cells were seeded on coverslips overnight and transfected with GFP, GFP-DLC1-WT or GFP-DLC1-Del(929-957) and incubated for 48 hours. Cells were then fixed with 4 % formaldehyde at room temperature (RT) for 10 min. After rinsing with PBS, cells were permeabilized by 0.2 % TritonX-100 (Sigma-Aldrich, Saint Louis, MO) for 10 min. Cells were blocked with 10% Goat serum for 1 hour at room temperature. Coverslips were stained with 1:50 anti-DLC1 rabbit polyclonal antibody 428, anti-CAV1 (BD Biosciences, San Jose, CA) 1:50 or anti-Myosin Light Chain Ser-19 (Cell Signaling Technology, Danvers, MA) 1:50 for 2h at RT followed by anti-Rabbit Alexa568 (1:250 dilution) or anti-Mouse Alexa488-conjugated secondary antibody (1:250 dilution) (Molecular Probes Inc, Eugene, OR), mounted with DAPI (Invitrogen, Carlsbad, CA), and visualized with a Zeiss 510 confocal microscope. For Phalloidin staining, cells were incubated in Rodanmine-Phallodin in PBS (1:50) (Molecular Probe, Carlsbad, CA) for 30 min followed by washing with PBS, stained with DAPI, and mounted.

Cell migration, Soft agar, and Clonogenic assays

Cell migration was measure by 6.5mm-diameter Falcon Cell culture inserts (8 μm pore size; Becton Dickinson). Transiently transfected cells or stable clones were trypsinized, resuspended in serum free RPMI medium 1640, and transferred to the upper chamber (7.5 × 10^4 cells in 300 μl). Six hundred μl 10% FBS in RPMI 1640 was placed in the lower chamber. After an 18-hour incubation, the cells remaining on the upper surface of insert were removed five times with a cotton swab moistened in PBS. Migrated cells on the lower surface were fixed in Methanol for 10 min at RT followed by staining with 2% crystal violet (Sigma-Aldrich, Saint Louis, MO) in methanol for 20 min, distained, examined, and

photographed by microscopy. For quantification, migrated cells were solubilized with 1% Triton X-100 and counted in a spectrophotomer at OD590nm. For soft agar assays, a 0.6 % agar (BD Bioscience, San Diego, CA) base in RPMI 1640 medium was placed in 60 mm dishes for 1 hour at RT. Then 1×10^5 cells were mixed with 0.4 % agar in RPMI 1640 medium with 10 % FBS and placed over the 0.6 % agar base. Cells were grown for 2 3 weeks, and colonies photographed microscopically and quantified with a colony counter. For colonogenic assays, 5×10^4 cells were seeded in 6 well plates 48 hours after transfection and cultured in 0.8 μg/ml G418 RPMI 1640 medium with 10% FBS for 2 weeks. Colonies were fixed, stained with 4% Crystal violet, and counted.

In Vivo Pull-Down Assay, Co-Immunoprecipitation, and Immunoblotting

For in vivo Pull-down assay, 293 T cells were co-transfected with plasmids expressing GST or GST fusion proteins together with GFP-DLC1 constructs. At 48 hours after transfection, the cells were lysed with golden lysis buffer (GLB: 20 mM Tris, pH 7.9/137 mM NaCl/10% glycerol/1% Triton X-100/5 mM EDTA/1 mM EGTA/1 mM Na3VO4/10 mM NaF/1 mM sodium pyrophosphate/1 mM glycerophosphate/ protease inhibitor mixture tablet). The supernatants were collected and concentrations quantified with a BCA kit (Pierce, Rockford, IL). One milligram of protein from each cell extracts was used for pull-down assays by adding 20 μl of glutathione Sepharose-4B slurry (Amersham, Pittsburgh, PA) and rotating 3 hours at 4°C. The pellets were sequentially washed by GLB, high-salt HNTG (20mM Hepes/500 mM NaCl/0.1% Triton X-100/10% glycerol), low-salt HNTG (20 mM Hepes/150 mM NaCl/0.1% Triton X-100/10% glycerol), and incubated with 20 μl loading buffer followed by immunoblotting. For co-immunoprecipitation experiments, equal amounts of protein lysates were incubated with control IgG or specific antibodies. Thirty microliters of protein A/G slurry (Pierce, Rockford, IL) was added to each immune reaction and rotated overnight at 4°C. The pellets were then washed three times as above. After separating protein samples by SDS/PAGE, immunoblotting was used to detect protein signals with anti-GST (Santa Cruz Biotechnology, CA), DLC1 (BD Biosciences, San Jose, CA), CAV1 (BD Biosciences, San Jose, CA), Actin (Invotrogen, Carlsbad, CA), or GFP (Covance, Princeton, NJ). For each blot, horseradish peroxidase-conjugated antirabbit or anti-mouse IgG (Amersham, Pittsburgh, PA) was used for the second reaction at 1:10,000 dilution. Immunocomplexes were visualized with an ECL kit (Amersham, Pittsburgh, PA).

Rhotekin-Rho Binding Domain (RBD) Pull-Down Assays

To measure active Rho (RhoGTP), DLC1 wild type and mutants were transiently transfected into 293T cells. After 48 hrs, cell extracts were collected using MLB lysis buffer (Millipore Corporation, Bedford, MA). Equal amounts of protein lysates were used for the pull-down assay by Rhotekin RBD agarose (Millipore Corporation, Bedford, MA). The pellets were washed three times with lysis buffer, resuspended in sample buffer, and then separated by 15% SDS/PAGE. Anti–Rho-A antibody (Millipore Corporation, Bedford, MA) was used to detect Rho-A-GTP. The same assays were used for DLC1 stable clones derived from human NSCLC line H358 and the siRNA-transfected H1299 cell line.

Mouse tumorigenicity studies

The mouse studies were approved by the NCI Animal Care and Use Committee and were conducted in compliance with the approved protocols. Six week-old female athymic nu/nu nude mice were obtained from Charles River (Wilmington, MA). H358 human lung cancer cells stably expressing DLC1 wild type and mutants were washed with cold phosphate-buffered saline and diluted in 10^7/ml with serum-free medium and 100μl cell suspension were injected subcutaneously into each mouse. Each group has 10 mice. After 45 days, the mice were euthanized and tumors weighted.

Statistical Analysis

Whole-genome Exon Array expression data on 20 lung adenocarcinoma/adjacent normal lung normal paired specimens (n=40) was downloaded from the Gene Expression Omnibus repository GSE12236 (51). Expression data was analyzed using Partek Genomics Suite after Core Meta-Probeset filter and quantile normalization. Expression differences between tumor and adjacent normal tissues were assessed by 1-way ANOVA. Expression values for DLC1 and CAV1 were exported into GraphPad Prism, which was used for correlation analysis. Expression values for DLC1 and CAV1 from the 443 lung adenocarcinomas from the National Cancer Institute Director's Challenge cohort (52) was obtained from Oncomine 2.0. Dot plots and Kaplan Meier-plots were generated using GraphPad Prism 5.0. For Kaplan-Meier analysis, DLC1 and CAV1 were dichotomized into high and low groups based on median expression values, and 60 month survival was used as the endpoint. All reported p-values are two-sided. Statistical analysis was carried out using Student's t-test with the Prism program. A *P* value <0.05 was considered significant.

Results

DLC1 interacts and co-localizes with CAV1 in lung cancer cells

Previous studies indicated that a fraction of cellular DLC1 localizes to caveolae in a complex with CAV1 (13, 19). To confirm that endogenous DLC1 and CAV1 co-localize and form a complex in lung cancer cells, we performed immunofluorescence and immunoprecipitation assays, respectively. Immunomicroscopy indicated extensive co-localization between endogenous DLC1 and CAV1 at the plasma membrane in two non-small cell lung cancer (NSCLC) lines, H1299 and H1703 (Fig. 1A). Co-immunoprecipation and western blotting assay confirmed complex formation between DLC1 and CAV1 in the cell lines (Fig. 1B). Following transfection of a plasmid encoding GFP-tagged full-length DLC1 (GFP-DLC1) into H727 cells, a NSCLC line that expresses readily detectable levels of CAV1 but has low levels of endogenous DLC1, co-immunoprecipitation showed a strong positive band (Fig. 1C).

Complex formation with CAV1 maps to the DLC1 START domain

To map the region of DLC1 required for complex formation with CAV1, plasmids encoding GFP-tagged full-length DLC1 (GFP-DLC1-WT) and various GFP-tagged DLC1 fragments were co-transfected into HEK 293T cells with a GST-CAV1-expression plasmid, pulled down by glutathione-coated beads, and western blotted with GFP antibodies. The DLC1

fragments were numbered according to their respective encoded N-terminal and C-terminal amino acid (Fig. 2A). Consistent with previous cytological data (19), complex formation was localized to the ~600 C-terminal amino acids, since DLC1 fragment pull-down resulted from GFP-DLC1-WT and GFP-DLC1(500-1091), while GFP-DLC1(1-492) did not bind GST-CAV1 (Fig. 2B). Complex formation was independent of the DLC1 RhoGAP activity, since a "GAP-dead" DLC1 mutant (R718A) also bound GST-CAV1, although it failed to inactivate RhoA (Supplementary Fig. 1A and B). Earlier studies predicted that amino acids 617-624 mediate DLC1-CAV1 complex formation (13). However, binding to CAV1 was preserved in a C-terminal fragment from which this sequence had been deleted [GFP-DLC1(500-1091)-Del(617-624)] (Fig. 2C). In addition, a C-terminal DLC1 fragment composed of amino acids 623-1091 gave a strong positive signal, while two internal DLC1 fragments, one spanning amino acids 500-638 and the other 609-878, which includes the entire RhoGAP domain, did not bind GST-CAV1 (Fig. 2B).

These results suggested that sequences C-terminal to amino acid 878 were responsible for DLC1 binding, implying that the START domain, which spans amino acids 879-1080, is required for binding. To identify smaller regions of DLC1 fragments that might be sufficient for binding GST-CAV1, we generated three C-terminal DLC1 fragments, each of which spanned about 100 non-overlapping amino acids. DLC1(899-996) showed strong binding to GST-CAV1, while weak binding was observed with DLC1(799-898), and no binding with DLC1(996-1091) (Fig. 2D). These results suggest that sequences within 899-996 of the START domain are required for complex formation.

To develop DLC1 mutants with lesions in the START domain that are deficient for binding CAV1, we deleted DLC1 amino acids 799-898 in full-length DLC1 [GFP-DLC1-Del(899-996)] and constructed three additional mutants from which about 30 of these amino acids had been deleted [GFP-DLC1-Del(899-928), GFP-DLC1-Del(929-957), and GFP-DLC1-Del(957-996)] (Fig 3A). When these mutants were transfected into HEK 293T cells, immunoprecipitation of endogenous CAV1 followed by anti-DLC1 western blotting demonstrated reduced binding for all the mutants when compared with the GFP-DLC1 wild type control (Fig. 3B). Binding to CAV1 was completely abrogated by the large deletion (899-996) and deletion of amino acids 929-957.

We focused on the GFP-DLC1-Del(929-957) mutant, since it had a small deletion and was severely deficient for complex formation. Because its stability was somewhat less than that of wild type GFP-DLC1, cells were transfected with a larger amount of this mutant DNA. Consistent with its inability to binding CAV1 in HEK 293T cells, the DLC1 mutant also co-localized less efficiently with GST-CAV1 when it was transfected into the A549 NSCLC line (Fig. 3C). In addition, immunofluorescent staining of A549 cells showed wild type GFP-DLC1 (green) and endogenous CAV1 (red) co-localized in punctate membrane-associated structures, while their co-localization was decreased in cells expressing the deletion mutant (Fig. 3D). These observations imply that the deleted DLC1 amino acids are required for efficient complex formation and co-localization with CAV1.

DLC1-Del(929-957) is deficient for suppression of cell migration and neoplastic growth

To evaluate the effect of CAV1 binding on biological and RhoGAP activities attributable to DLC1, A549 cells were transiently transfected with the GFP-DLC1-Del(929-957) mutant and examined in several bioassays and for RhoGTP. The mutant was severely deficient in its ability to reduce cell growth in soft agar, clonogenic growth, and cell migration, compared with the activity of wild type DLC1, although the transfectants expressed similar levels of wild type and mutant protein (Fig. 4A-C, p<0.05). Despite the lower biological activity of the mutant, it reduced the level of active Rho as efficiently as wild type DLC1 in A549 cells (Fig. 4D) and in a second NSCLC line, H1299 (Supplementary Fig. 1B).

The H358 NSCLC line, with low endogenous DLC1, was stably transfected with wild type DLC1 and the DLC1-Del(929-957) mutant. Similar to the results with transient transfection of A549, the stable mutant in H358 was deficient in several bioassays, including growth in soft agar, cell migration, and xenograft formation in nude mice, although it reduced active RhoGTP with the efficiency similar to wild type (Fig. 5A-D, p<0.05). Consistent with the low levels of active Rho induced by the mutant, stress fiber formation, which is a Rho-dependent activity, was reduced to a similar degree in cells expressing the wild type and mutant DLC1 proteins (Supplementary Fig. 1C).

Taken together, the results indicate that the interaction of DLC1 with CAV1 inhibited migratory and tumorigenic phenotypes in NSCLC. Indeed, siRNA-mediated knock-down of CAV1 in H1299 cells, which expresses readily detectable levels of endogenous CAV1 and DLC1, led to an increase in cell migration consistent with CAV1 being growth inhibitory for this line (Supplementary Fig. 2A, B). Analogous observations were made upon siRNA-mediated knock-down of DLC1 was used (Supplementary Fig. 2A, B). When the siRNAs against both genes were used together, there was no further increase in migration rate.

DLC1 and CAV1 expression levels are positively correlated; low DLC1 predicts a poor prognosis

When the relative levels of endogenous DLC1 and CAV1 were compared in a panel of NSCLC lines, they appeared to correlate with each other. By western blotting, both proteins were readily detected in H157, H1299 and H1703 cells, while there was low or no expression of either protein in H322, H358, A549 or H727 cells (Fig. 6A). This observation suggested that DCL1 and CAV1 might be co-regulated in primary NSCLC. To examine this possibility, we analyzed a publicly available dataset featuring mRNA expression profiles of 20 paired specimens of lung adenocarcinoma and adjacent normal lung (20), which confirmed DLC1 and CAV1 were down-regulated in tumor tissue compared to paired normal adjacent lung (FDR-corrected p<0.001) (Fig. 6B). Furthermore, expression values of DLC1 and CAV1 in tumor tissues were positively correlated (Spearmen r=0.45, p<0.05) (Fig. 6C).

Expression values of DLC1 and CAV1 were also positively correlated in a larger dataset of lung adenocarcinoma expression profiles, from the National Cancer Institute Director's Challenge Cohort (Fig. 6D). Interestingly, low expression of DLC1 was associated with a poor prognosis in these patients (Fig. 6E). However, there was no prognostic significance

associated with the level of CAV1 (Supplementary Fig. 3A-C), and the combination of CAV1 and DLC1 levels did not enhance the predictive power of DLC1 alone (Fig. 6F).

Discussion

High levels of active RhoA and RhoC are found in many cancers, and may be associated with a poor prognosis (21, 22). Rho activity is regulated by three classes of genes: guanine nucleotide exchange factors (GEFs), which activate Rho, GTPase accelerating proteins (GAPs), which inactivate Rho, and guanine nucleotide dissociation inhibotors (GDIs), which sequester inactive Rho in the cytoplasm (23, 24). In contrast to the frequently mutated Ras genes, Rho is rarely, if ever, mutated in cancer. Instead, increased Rho activity in cancer may be attributable to increased expression of RhoA or RhoC, increased expression or mutation of Rho GEFs, increased or decreased expression of Rho GDIs, depending on whether they contribute positively or negatively, respectively, to a given tumor, or decreased RhoGAP activity.

There are several Rho GAPs whose major enzymatic activity regulates RhoA (and RhoC, where it has been examined), including DLC1-3, p190RhoGAP, p73RhoGAP, GMIP, and PARG1. In contrast to the other Rho GAPs, DLC1-3 are frequently inactivated in tumors, via homozygous deletion, promoter methylation, or point mutation (5, 25, 26). This observation has suggested that the DLC proteins may possess other functions, in addition to their RhoGAP activity, that contribute to tumor suppression, which may help explain the preferential inactivation of DLC genes in cancer. As noted in the Introduction, DLC1 binds physiologically to several proteins and this binding is required for the full biological activity of DLC1. Here, we have focused on complex formation between DLC1 and CAV1 (13, 19), mapping the DLC1 sequences required for complex formation, and studying the biological activity of a DLC1 mutant deficient for complex formation with CAV1. Our experimental analysis focused on NSCLC lines because DLC1 expression is frequently down-regulated in these tumors.

After demonstrating complex formation between endogenous DLC1 and CAV1 and their co-localization in caveolae, we mapped the DLC1 sequences required for complex formation with CAV1. This analysis indicated a necessary and sufficient role of the START domain for this interaction. A prior study with the rat homolog of DLC1 had used microscopy to infer the importance of the GAP domain for interaction with CAV1 (19), but, using a biochemical assay, we did not detect complex formation between the human DLC1 GAP domain and CAV1.

The DLC1-Del(929-957) mutant, which is missing 30 amino acids from the START domain, was found to be deficient for complex formation with CAV1, for co-localization with CAV1 by microscopy, and for the suppression of cell migration and growth in several bioassays. However, the RhoGAP activity of the mutant in cells, as determined by the level of active Rho in cell extracts, was not attenuated in cells expressing DLC1 mutant deficient for CAV1 binding. Since the START domain of DLC1 is located C-terminal to the RhoGAP domain, this result implies that the START domain is not a major regulator of DLC1 RhoGAP activity in cells. Similar results were seen with microscopy of the H358 NSCLC line stably

transfected with the CAV1-deficient binding mutant. The reduced biological activity of the mutant, despite its efficient reduction of active Rho and Rho-associated activity, means that a RhoGAP-independent mechanism must account for the contribution of complex formation between DLC1 and CAV1 to the biological activity of DLC1, in contrast to a previous speculation (13). An analogous phenotype has been reported previously for DLC1 mutants deficient for binding tensins or talin and FAK; the mutations in those instances were located in DLC1 sequences N-terminal to the RhoGAP domain (11, 14).

As noted in the Introduction, CAV1 may promote or inhibit tumor development, depending on the cellular context (18). Several groups have reported that CAV1 protein levels are up-regulated in bladder, esophageal, prostate, and hepatocellular cancer (27-33). However, CAV1 expression is consistently down-regulated in other malignancies, such as ovarian, and breast cancers (34). CAV1 expression may be increased in squamous cell carcinoma of the lung, but it is decreased in adenocarcinoma, in comparison to normal lung tissue (35-38). Consistent with those observations, we found that the siRNA-mediated knockdown of endogenous CAV1 in the H1299 adenocarcinoma NSCLC line was associated with an increase in cell migration, although the opposite effect was reported previously with another derivative of this cell line, perhaps because of a difference in passage history or culture conditions (39). As expected, an increase in migration was seen when a DLC1 siRNA reduced the level of endogenous DLC1 in the line. Since there was no further increase in migration rate when both CAV1 and DLC1 were reduced when the siRNAs were used together, we speculate that CAV1 and DLC1 may contribute to the same pathway that regulates cell migration, although other interpretations are possible. In this context, complex formation between DLC1 and CAV1 might increase the tumor suppressive activity of CAV1, which could account, at least in part, for the reduced tumor suppressive activity of the 929-957 DLC1 mutant.

The 15 human proteins with START domains have been divided phylogenetically into six classes, with the DLC1-3 proteins representing a distinct class (8, 9). The class that is composed of StarD1 and StarD3 and the one composed of StarTD4-6 are involved in the metabolism and transport of cholesterol, and cholesterol is the ligand for their START domains (40). The ligands for a third class, which comprises StarD2, StarD7, and StarD10-11, have also been identified as lipids (41-44). These include phosphatidylcholine for STARD2 and STARD7, phosphatidylcholine and phosphatidylethanolamine for STARD10, and ceramide for STARD11. The ligands for the other three classes, including the one composed of DLC1-3, have not been identified.

We speculate the molecular model for StarD2 function may be relevant to the interaction identified here between the START domain of DLC1 and CAV1 (Kanno, Wu et al. 2007). While most START-containing proteins are multidomain proteins, StarD2 is composed of only a START domain. However, StarD2 participates in protein-protein interactions, but they depend on phosphotidylcholine binding to StarD2. If the START domain of DLC1 functions in an analogous manner, a lipid whose identity remains to be determined probably mediates complex formation with CAV1. The fact that CAV1 is found in caveolae, which are lipid-rich domains, increases the plausibility of this speculation.

We also identified a correlation between the relative expression of DLC1 and CAV1 in a panel of NSCLC lines, and confirmed a similar correlation in primary NSCLC adenocarcinomas from two publicly available datasets. In the larger dataset, which was composed of more than 400 adenocarcinomas, low levels of DLC1 expression were found to predict an adverse outcome. This result is consistent with a previous report in lung cancer that the degree of DLC1 methylation was inversely correlated with the extent of disease (45). A recent report also identified low DLC1 expression as a poor prognostic factor in oral squamous cell cancer (46). The results suggest DLC1 inactivation contributes to cancer progression, probably via the combined effects of its RhoGAP-dependent and RhoGAP-independent activities.

Supplementary Material

Refer to Web version on PubMed Central for supplementary material.

Acknowledgments

References

1. Yuan BZ, Miller MJ, Keck CL, Zimonjic DB, Thorgeirsson SS, Popescu NC. Cloning, characterization, and chromosomal localization of a gene frequently deleted in human liver cancer (DLC-1) homologous to rat RhoGAP. Cancer Res. 1998; 58:2196–9. [PubMed: 9605766]

2. Liao YC, Lo SH. Deleted in liver cancer-1 (DLC-1): a tumor suppressor not just for liver. Int J Biochem Cell Biol. 2008; 40:843–7. [PubMed: 17521951]

3. Durkin ME, Yuan BZ, Zhou X, et al. DLC-1:a Rho GTPase-activating protein and tumour suppressor. J Cell Mol Med. 2007; 11:1185–207. [PubMed: 17979893]

4. Zhong D, Zhang J, Yang S, et al. The SAM domain of the RhoGAP DLC1 binds EF1A1 to regulate cell migration. J Cell Sci. 2009; 122:414–24. [PubMed: 19158340]

5. Kim TY, Vigil D, Der CJ, Juliano RL. Role of DLC-1, a tumor suppressor protein with RhoGAP activity, in regulation of the cytoskeleton and cell motility. Cancer Metastasis Rev. 2009; 28:77–83. [PubMed: 19221866]

6. Wong CM, Yam JW, Ching YP, et al. Rho GTPase-activating protein deleted in liver cancer suppresses cell proliferation and invasion in hepatocellular carcinoma. Cancer Res. 2005; 65:8861–8. [PubMed: 16204057]

7. Holeiter G, Heering J, Erlmann P, Schmid S, Jahne R, Olayioye MA. Deleted in liver cancer 1 controls cell migration through a Dia1-dependent signaling pathway. Cancer Res. 2008; 68:8743–51. [PubMed: 18974116]

8. Alpy F, Tomasetto C. Give lipids a START: the StAR-related lipid transfer (START) domain in mammals. J Cell Sci. 2005; 118:2791–801. [PubMed: 15976441]

9. Clark BJ. The mammalian START domain protein family in lipid transport in health and disease. J Endocrinol.

10. Liao YC, Si L, deVere White RW, Lo SH. The phosphotyrosine-independent interaction of DLC-1 and the SH2 domain of cten regulates focal adhesion localization and growth suppression activity of DLC-1. J Cell Biol. 2007; 176:43–9. [PubMed: 17190795]

11. Qian X, Li G, Asmussen HK, et al. Oncogenic inhibition by a deleted in liver cancer gene requires cooperation between tensin binding and Rho-specific GTPase-activating protein activities. Proc Natl Acad Sci U S A. 2007; 104:9012–7. [PubMed: 17517630]

12. Chan LK, Ko FC, Ng IO, Yam JW. Deleted in liver cancer 1 (DLC1) utilizes a novel binding site for Tensin2 PTB domain interaction and is required for tumor-suppressive function. PLoS One. 2009; 4:e5572. [PubMed: 19440389]

13. Yam JW, Ko FC, Chan CY, Jin DY, Ng IO. Interaction of deleted in liver cancer 1 with tensin2 in caveolae and implications in tumor suppression. Cancer Res. 2006; 66:8367–72. [PubMed: 16951145]

14. Li G, Du X, Vass WC, Papageorge AG, Lowy DR, Qian X. Full activity of the deleted in liver cancer 1 (DLC1) tumor suppressor depends on an LD-like motif that binds talin and focal adhesion kinase (FAK). Proc Natl Acad Sci U S A. 108:17129–34.

15. Yang X, Popescu NC, Zimonjic DB. DLC1 interaction with S100A10 mediates inhibition of in vitro cell invasion and tumorigenicity of lung cancer cells through a RhoGAP-independent mechanism. Cancer Res. 71:2916–25.

16. Yang XY, Guan M, Vigil D, Der CJ, Lowy DR, Popescu NC. p120Ras-GAP binds the DLC1 Rho-GAP tumor suppressor protein and inhibits its RhoA GTPase and growth-suppressing activities. Oncogene. 2009; 28:1401–9. [PubMed: 19151751]

17. Glenney JR Jr. Tyrosine phosphorylation of a 22-kDa protein is correlated with transformation by Rous sarcoma virus. J Biol Chem. 1989; 264:20163–6. [PubMed: 2479645]

18. Goetz JG, Lajoie P, Wiseman SM, Nabi IR. Caveolin-1 in tumor progression: the good, the bad and the ugly. Cancer Metastasis Rev. 2008; 27:715–35. [PubMed: 18506396]

19. Yamaga M, Sekimata M, Fujii M, et al. A PLCdelta1-binding protein, p122/RhoGAP, is localized in caveolin-enriched membrane domains and regulates caveolin internalization. Genes Cells. 2004; 9:25–37. [PubMed: 14723705]

20. Xi L, Feber A, Gupta V, et al. Whole genome exon arrays identify differential expression of alternatively spliced, cancer-related genes in lung cancer. Nucleic Acids Res. 2008; 36:6535–47. [PubMed: 18927117]

21. Ellenbroek SI, Collard JG. Rho GTPases: functions and association with cancer. Clin Exp Metastasis. 2007; 24:657–72. [PubMed: 18000759]

22. Karlsson R, Pedersen ED, Wang Z, Brakebusch C. Rho GTPase function in tumorigenesis. Biochim Biophys Acta. 2009; 1796:91–8. [PubMed: 19327386]

23. Vigil D, Cherfils J, Rossman KL, Der CJ. Ras superfamily GEFs and GAPs: validated and tractable targets for cancer therapy? Nat Rev Cancer. 10:842–57.

24. Garcia-Mata R, Boulter E, Burridge K. The 'invisible hand': regulation of RHO GTPases by RHOGDIs. Nat Rev Mol Cell Biol. 12:493–504.

25. Durkin ME, Ullmannova V, Guan M, Popescu NC. Deleted in liver cancer 3 (DLC-3), a novel Rho GTPase-activating protein, is downregulated in cancer and inhibits tumor cell growth. Oncogene. 2007; 26:4580–9. [PubMed: 17297465]

26. Liao YC, Shih YP, Lo SH. Mutations in the focal adhesion targeting region of deleted in liver cancer-1 attenuate their expression and function. Cancer Res. 2008; 68:7718–22. [PubMed: 18829524]

27. Rajjayabun PH, Garg S, Durkan GC, Charlton R, Robinson MC, Mellon JK. Caveolin-1 expression is associated with high-grade bladder cancer. Urology. 2001; 58:811–4. [PubMed: 11711373]

28. Fong A, Garcia E, Gwynn L, Lisanti MP, Fazzari MJ, Li M. Expression of caveolin-1 and caveolin-2 in urothelial carcinoma of the urinary bladder correlates with tumor grade and squamous differentiation. Am J Clin Pathol. 2003; 120:93–100. [PubMed: 12866378]

29. Hu YC, Lam KY, Law S, Wong J, Srivastava G. Profiling of differentially expressed cancer-related genes in esophageal squamous cell carcinoma (ESCC) using human cancer cDNA arrays: overexpression of oncogene MET correlates with tumor differentiation in ESCC. Clin Cancer Res. 2001; 7:3519–25. [PubMed: 11705871]

30. Kato K, Hida Y, Miyamoto M, et al. Overexpression of caveolin-1 in esophageal squamous cell carcinoma correlates with lymph node metastasis and pathologic stage. Cancer. 2002; 94:929–33. [PubMed: 11920460]

31. Yang G, Truong LD, Timme TL, et al. Elevated expression of caveolin is associated with prostate and breast cancer. Clin Cancer Res. 1998; 4:1873–80. [PubMed: 9717814]

32. Satoh T, Yang G, Egawa S, et al. Caveolin-1 expression is a predictor of recurrence-free survival in pT2N0 prostate carcinoma diagnosed in Japanese patients. Cancer. 2003; 97:1225–33. [PubMed: 12599229]

33. Tse EY, Ko FC, Tung EK, et al. Caveolin-1 Overexpression is Associated With Hepatocellular Carcinoma Tumorigenesis and Metastasis. J Pathol.

34. Razani B, Lisanti MP. Caveolin-deficient mice: insights into caveolar function human disease. J Clin Invest. 2001; 108:1553–61. [PubMed: 11733547]

35. Li M, Chen H, Diao L, Zhang Y, Xia C, Yang F. Caveolin-1 and VEGF-C promote lymph node metastasis in the absence of intratumoral lymphangiogenesis in non-small cell lung cancer. Tumori. 96:734–43. [PubMed: 21302621]

36. Kopantzev EP, Monastyrskaya GS, Vinogradova TV, et al. Differences in gene expression levels between early and later stages of human lung development are opposite to those between normal lung tissue and non-small lung cell carcinoma. Lung Cancer. 2008; 62:23–34. [PubMed: 18394749]

37. Yoo SH, Park YS, Kim HR, et al. Expression of caveolin-1 is associated with poor prognosis of patients with squamous cell carcinoma of the lung. Lung Cancer. 2003; 42:195–202. [PubMed: 14568687]

38. Kato T, Miyamoto M, Kato K, et al. Difference of caveolin-1 expression pattern in human lung neoplastic tissue. Atypical adenomatous hyperplasia, adenocarcinoma and squamous cell carcinoma. Cancer Lett. 2004; 214:121–8. [PubMed: 15331180]

39. Shatz M, Lustig G, Reich R, Liscovitch M. Caveolin-1 mutants P132L and Y14F are dominant negative regulators of invasion, migration and aggregation in H1299 lung cancer cells. Exp Cell Res. 316:1748–62.

40. Lavigne P, Najmanivich R, Lehoux JG. Mammalian StAR-related lipid transfer (START) domains with specificity for cholesterol: structural conservation and mechanism of reversible binding. Subcell Biochem. 51:425–37.

41. Hanada K, Kumagai K, Yasuda S, et al. Molecular machinery for non-vesicular trafficking of ceramide. Nature. 2003; 426:803–9. [PubMed: 14685229]

42. Olayioye MA, Vehring S, Muller P, et al. StarD10, a START domain protein overexpressed in breast cancer, functions as a phospholipid transfer protein. J Biol Chem. 2005; 280:27436–42. [PubMed: 15911624]

43. Kanno K, Wu MK, Agate DS, et al. Interacting proteins dictate function of the minimal START domain phosphatidylcholine transfer protein/StarD2. J Biol Chem. 2007; 282:30728–36. [PubMed: 17704541]

44. Horibata Y, Sugimoto H. StarD7 mediates the intracellular trafficking of phosphatidylcholine to mitochondria. J Biol Chem. 285:7358–65.

45. Castro M, Grau L, Puerta P, et al. Multiplexed methylation profiles of tumor suppressor genes and clinical outcome in lung cancer. J Transl Med. 8:86. [PubMed: 20849603]

46. Tripathi SC, Kaur J, Matta A, et al. Loss of DLC1 is an independent prognostic factor in patients with oral squamous cell carcinoma. Mod Pathol.

47. Qian X, Li G, Vass WC, et al. The Tensin-3 protein, including its SH2 domain, is phosphorylated by Src and contributes to tumorigenesis and metastasis. Cancer Cell. 2009; 16:246–58. [PubMed: 19732724]

48. Anborgh PH, Qian X, Papageorge AG, Vass WC, DeClue JE, Lowy DR. Ras-specific exchange factor GRF: oligomerization through its Dbl homology domain and calcium-dependent activation of Raf. Mol Cell Biol. 1999; 19:4611–22. [PubMed: 10373510]

49. Buck CB, Pastrana DV, Lowy DR, Schiller JT. Efficient intracellular assembly of papillomaviral vectors. J Virol. 2004; 78:751–7. [PubMed: 14694107]

50. Shedden K, Taylor JM, Enkemann SA, et al. Gene expression-based survival prediction in lung adenocarcinoma: a multi-site, blinded validation study. Nat Med. 2008; 14:822–7. [PubMed: 18641660]

51. http://www.ncbi.nlm.nih.gov/geo/

52. https://array.nci.nih.gov/caarray/project/details.action?project.experiment.publicIdentifier=jacob-00182
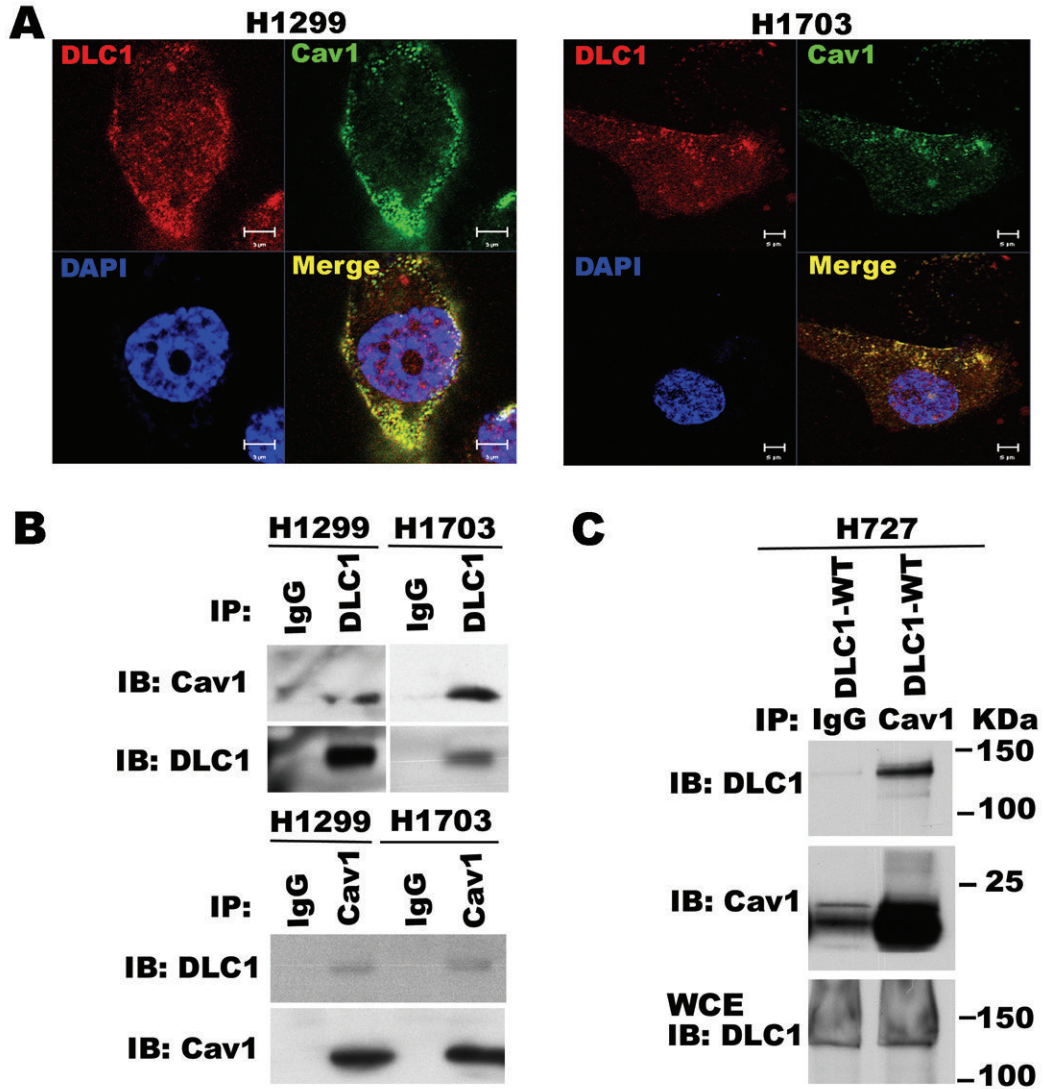
Figure 1.
DLC1 and CAV1 form a complex in lung cancer cells. (A) DLC1 and CAV1 were double stained with rabbit anti-DLC1 (1:50) and mouse anti-CAV1 (1:50) antibodies followed by Alexaflor 568 and Alexaflor 466. Nuclei were stained with propidium iodide. DLC1 and CAV1 partially co-localized in the membrane of H1299 and H1703 cells. Scale bars represent 5 μm. (B) Extracts from H1299 and H1703 cells, which contain high levels of endogenous DLC1 and CAV1, were immunoprecipitated (IP) with control IgG, DLC1, or CAV1 antibody. Co-precipitated CAV1 or DLC1 proteins were detected by anti-CAV1 or anti-DLC1 antibody. (C) GFP vector or GFP-DLC1-WT was transfected into H727 cells, which has low endogenous DLC1 and readily detectable CAV1 protein. Immunoprecipitated by CAV1 followed by immunoblotting with GFP antibody showed GFP-DLC1-WT complex formation with CAV1 protein.
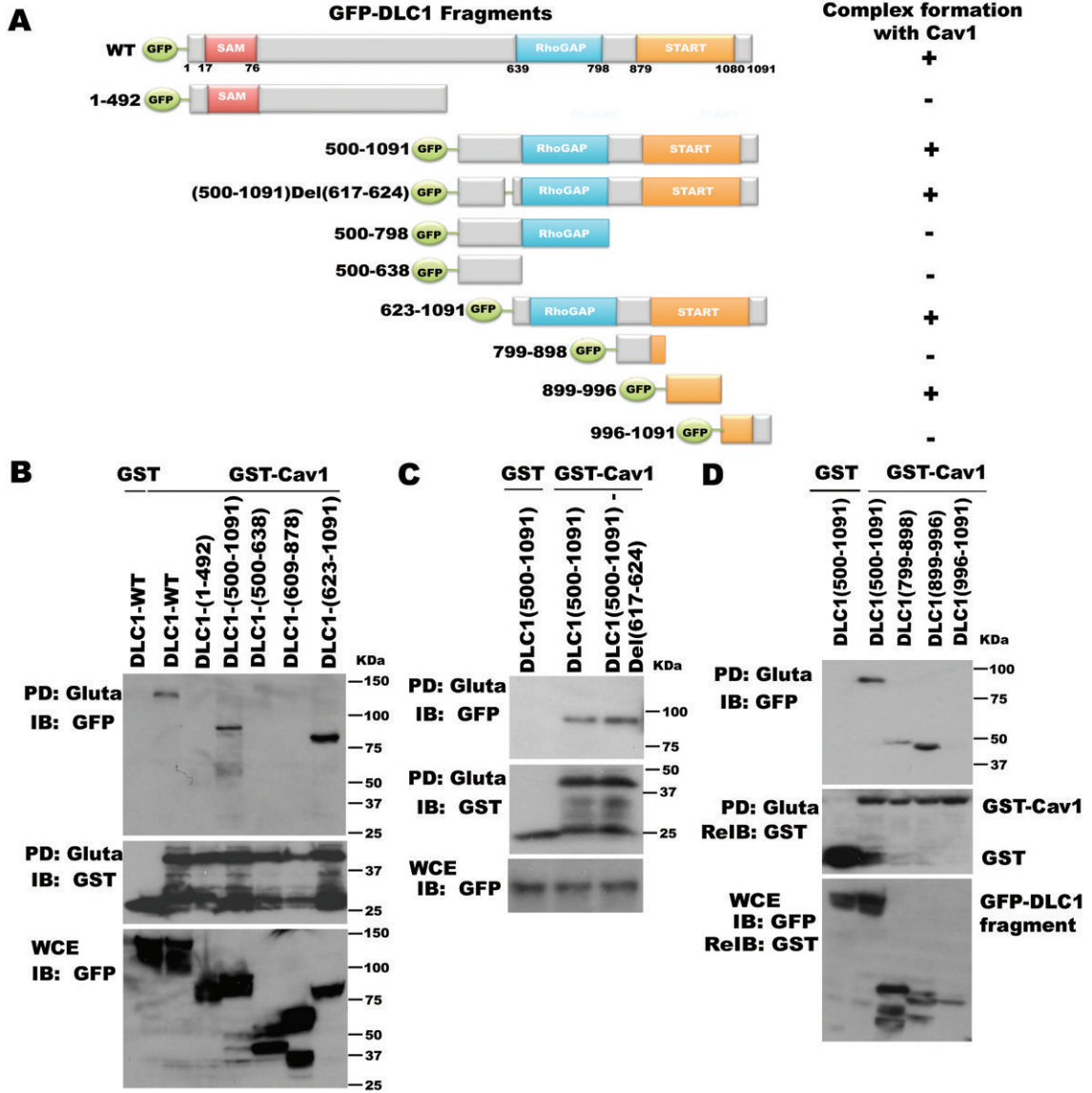
Figure 2.
Mapping the CAV1 interaction to the START domain in the C-terminus of DLC1. (A) Diagram of GFP-DLC1-WT full length and fragments of GFP-tagged DLC1 (left). Amino acid numbers are for human DLC1. "+" stands for positive complex formation between DLC1 and CAV1 in this study; "-" stands for weak or no complex formation between DLC1 and CAV1 in this study (right). (B) C-terminal of DLC1 sequence aa 623-1091 of DLC1 was necessary for complex formation between DLC1 and CAV1. 293T cells were co-transfected with GFP-DLC1-WT, GFP-DLC1(1-492), GFP-DLC1(500-1091), GFP-DLC1(500-638), GFP-DLC1(609-878), or GFP-DLC1(623-1091) and GST or GST-CAV1. After 48 hours, cells were lysed and pulled down by Sepharose-4B (Gluta) and immunoblotted (IB). WCE = whole cell extract. Cell extracts were used as a loading control. (C) Deletion of DLC1 amino acids 617-624 did not affect complex formation of DLC1 and CAV1 in 293T cells. (D) Mapping the START domain of DLC1 for CAV1 binding. GST-DLC1 START domain

fragments and GST or GST-CAV1 were co-transfected into 293T cells. After Gluta pull-down, DLC1 signal was detected with GFP antibody. GFP-DLC1(899-996) showed the strongest positive band.
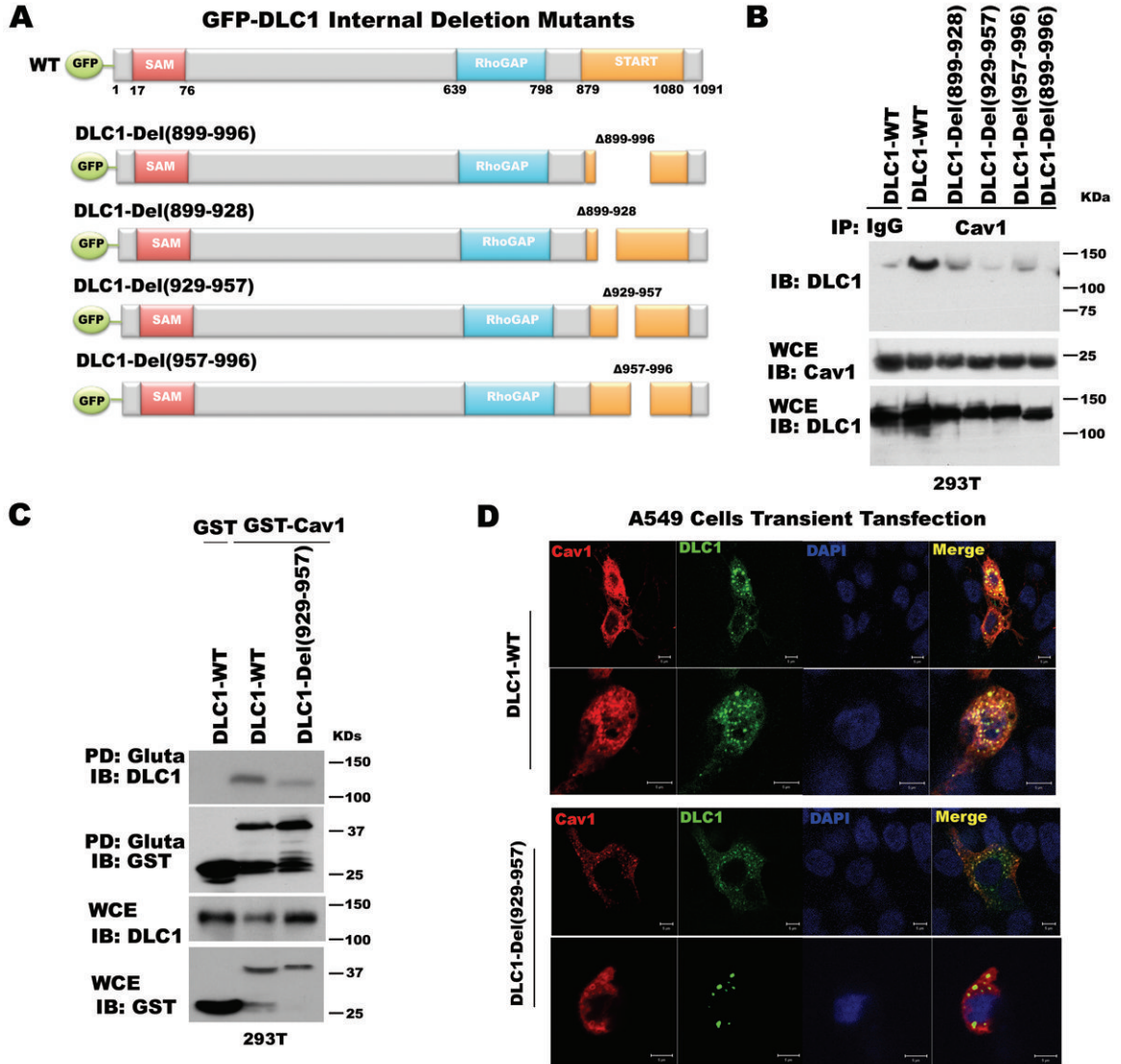
Figure 3.
(A) Domain structures of GFP-tagged deletions in full-length GFP-DLC1-WT. (B) To confirm amino acids 899-996 in DLC1 START domain is necessary for CAV1 binding, GFP-DLC1-WT and full-length mutants with deletions involving these START sequences were co-transfected into 293T cells. Equal amounts of protein were IP with IgG control or anti-CAV1 antibody, then IB with GFP antibody. Cell extracts were used as loading controls. (C) Full length GFP-DLC1-WT, GFP-DLC1-Del(929-957) and GST or GST-CAV1 were co-transfected into 293T cells. GST pull-down assay showed deletion of amino acid 929-957 abolished complex formation of DLC1 and CAV1. (D) Immunofluorescent staining of A549, which expresses very low levels of endogenous DLC1, transiently transfected with GFP-DLC1-WT and GFP-DLC1-Del(929-957). Representative photomicrographs show extensive co-localization with CAV1 in GFP-DLC1-WT expressing cells, which was decreased in GFP-DLC1-Del(929-927) expressing cells.
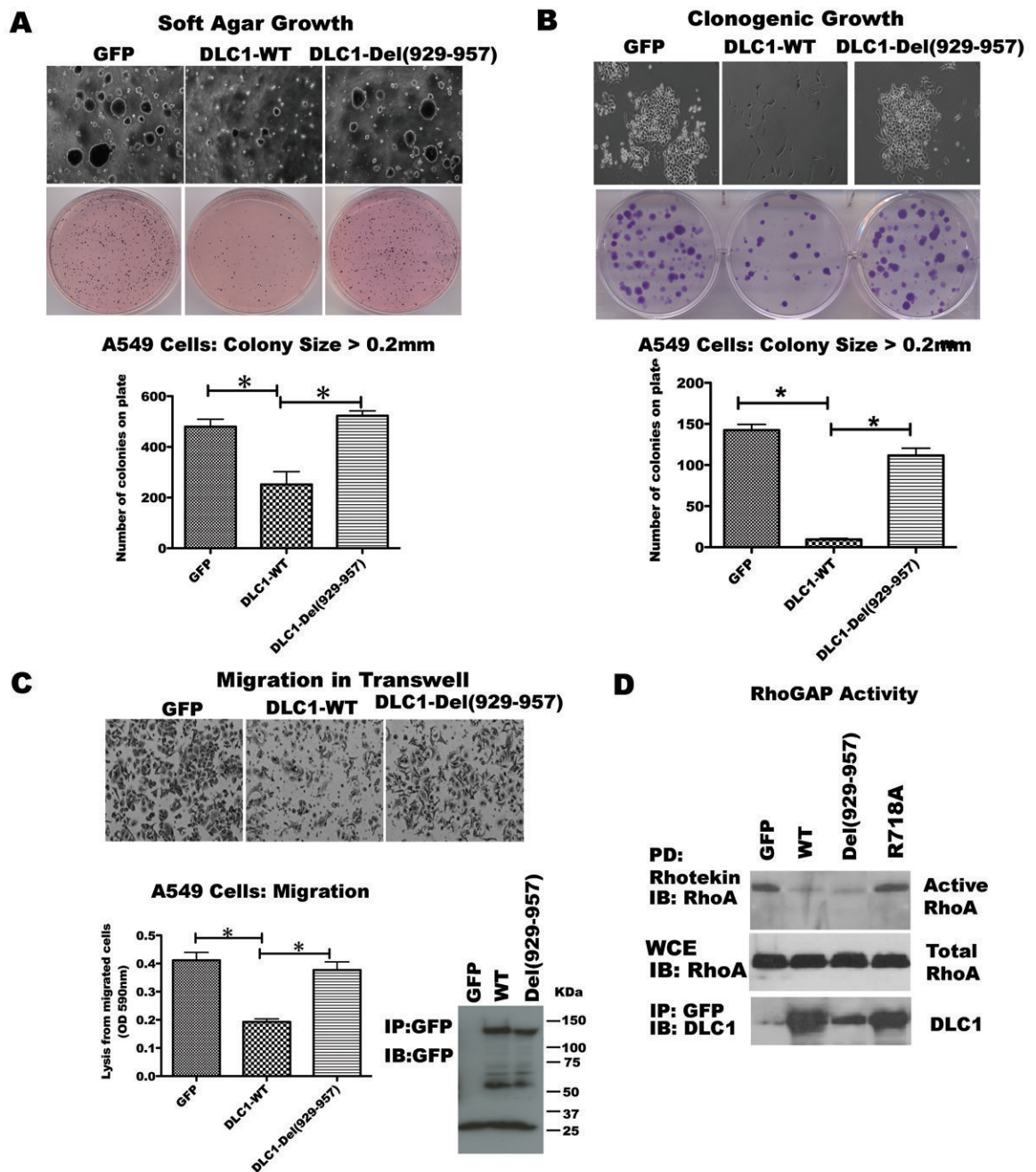
Figure 4.
Transient transfection of DLC1-Del (929-957) mutant inhibits colony growth in agar, clonogenic growth, and cell migration less efficiently than DLC1-WT in A549 cells. (A) Soft agar growth. After transfection of A549 cells for 24 hours, 1×10^6 cells were seeded in soft agar. Upper panels: Photographs were taken after incubation for 21 days. Lower panel: quantitation of agar colonies >0.2 mm. (B) Clonogenic growth. 5×10^4 cells were seeded on plates, cultured for 12 days in medium containing 0.8 mg/ml G418, G418-resistant colonies were stained with crystal violet, photographed (upper panels), and counted (lower panel). (C) Migration in transwell. 1×10^5 cells were seeded in a transwell dish, cultured for 18

hours, the migrated cells stained with crystal violet, photographed (upper panel), and quantified OD590 nm (lower panel). Inset: Western blot shows expression of GFP, DLC1-WT and DLC1-Del(929-957) in A549 cells 48 hours after transfection. These cells were used for the biological experiments in the figure. Columns: mean of three individual experiments; bars, SD; *, P<0.05. (D) RhoGAP activity. Active RhoA (RhoGTP) in A549 cells expressing WT- DLC1 or the indicated mutants were analyzed by Rhotekin pull-down assay followed by anti-RhoA blotting (upper panel). DLC1 expression and total RhoA loading controls were confirmed by immunoblotting (lower panels).
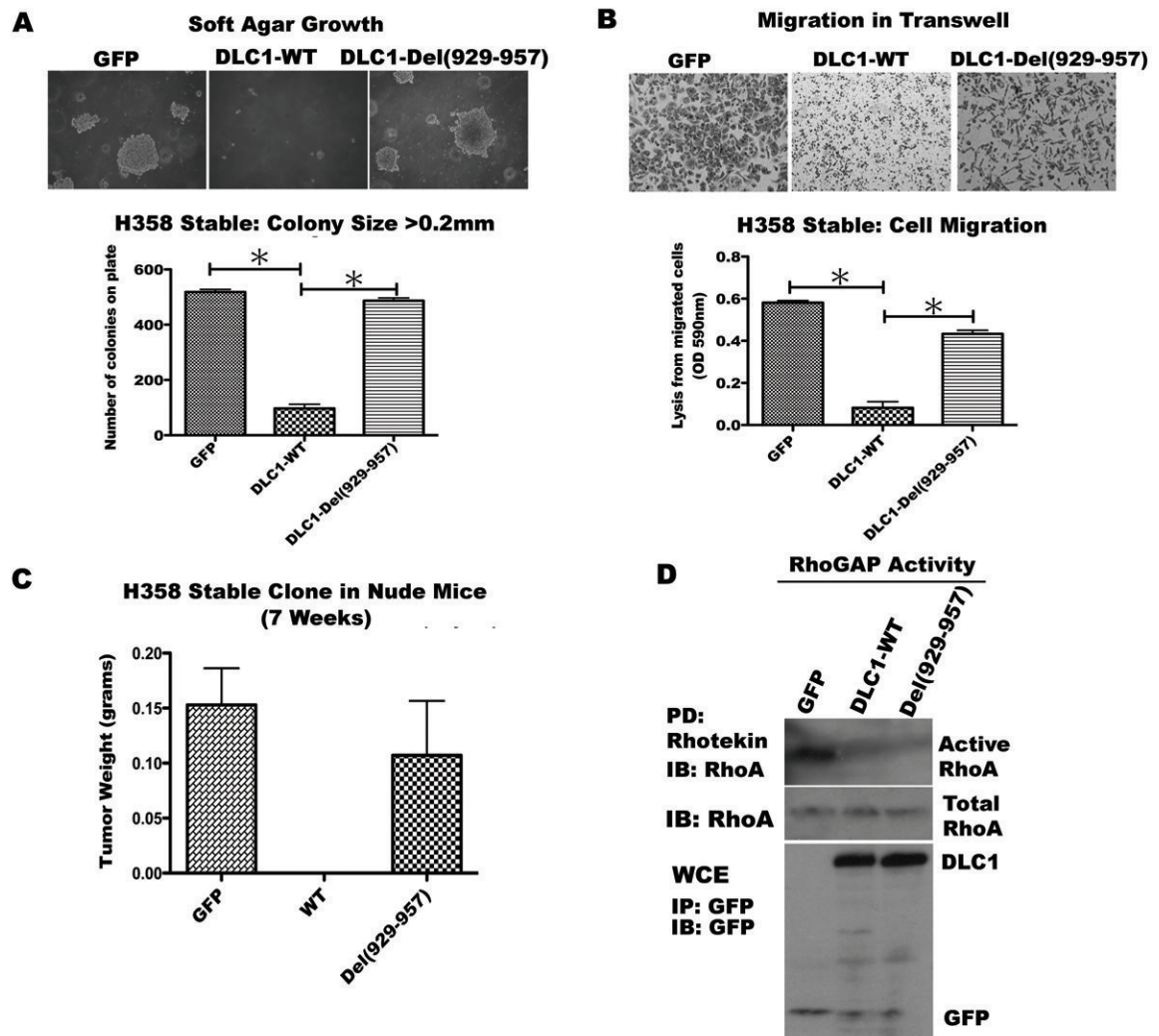
Figure 5.
H358 cells stably transfected with DLC1-Del(929-957) are deficient for suppression of agar growth, transwell migration, and xenograft tumor formation. (A) Agar growth. 1×10^6 of the indicated H358 stable clones were placed in soft agar, grown for 21 days, and photographed (upper panel) and counted (lower panel). (B) Transwell migration. 1×10^5 H358 cells were seeded in the transwell dish, cultured for 18 hours, the migrated cells stained with crystal violet and photographed (upper panel), and lysates xquantified at OD 590 mm. Columns: mean of three individual experiments; bars, SD; *, P<0.05. (C) Xenograft growth. Nude mice were injected subcutaneously with 1×10^6 H358 cells. Tumor weights were measured after sacrifice of the mice 7 weeks after injection. The data represent mean ± SE in each group (*, P < 0.01). (D) RhoGAP activity of DLC1-Del(929-957) mutant in H358 cells. DLC1, DLC1-WT, DLC1-Del(929-957) or R718A were analyzed by Rhotekin pull-down assay followed by anti-RhoA blotting (upper panel). The expression of DLC1 in the transiently transfected cells and total RhoA loading controls were confirmed by immunoblotting (lower panels).
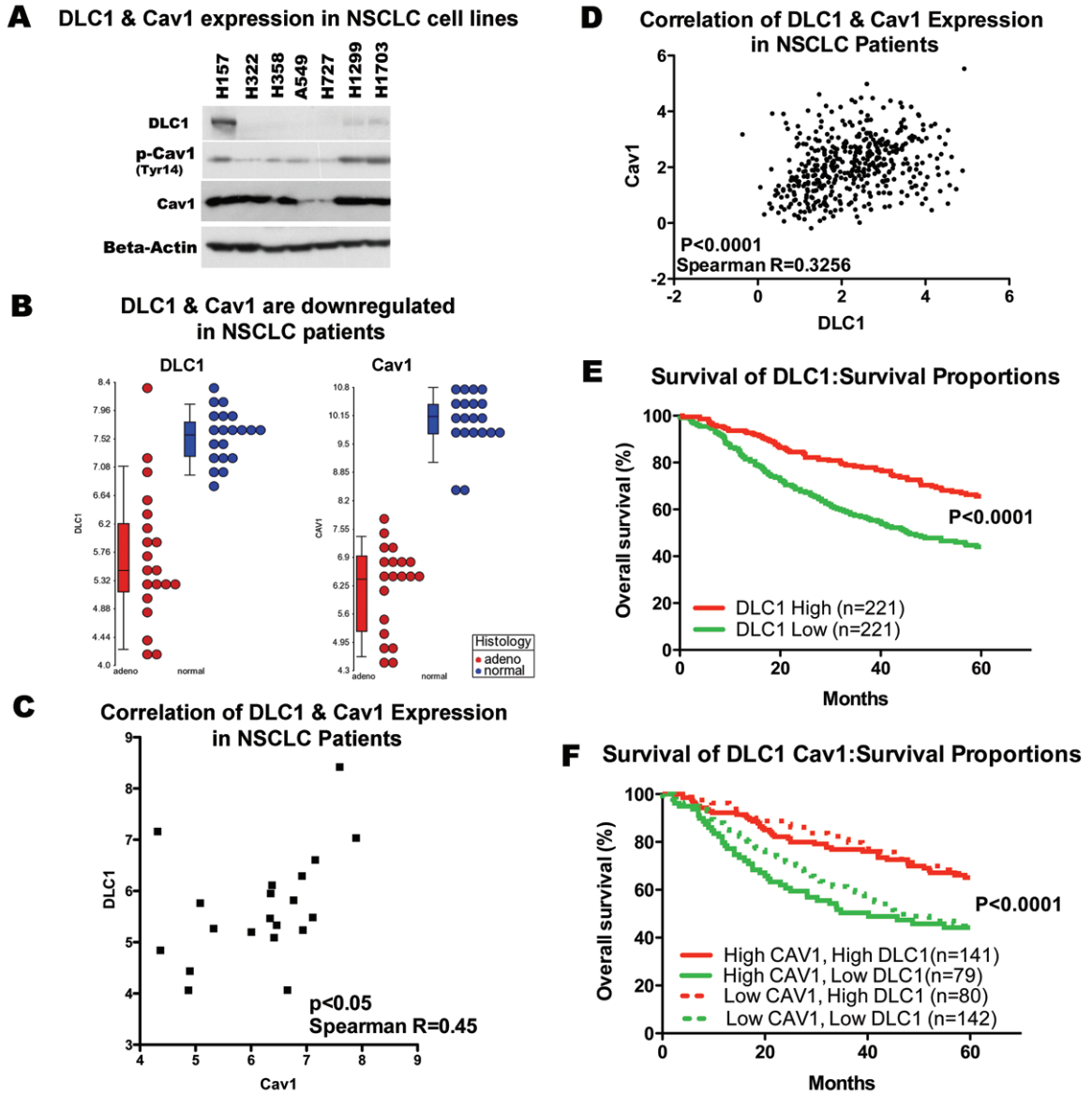
Figure 6.
DLC1 and CAV1 expression is positively correlated in lung cancer, and DLC1 expression has prognostic significance. (A) Immunoblotting analysis of DLC1, CAV1 and pCAV1(Tyr14) expression in lung cancer cell lines. The blot was probed with an anti-beta-actin antibody as a loading control. (B) Reduced DLC1 and CAV1 RNA expression in NSCLC. From whole-genome Exon Array expression analysis data, expression of DLC1 and CAV1 in NSCLC compared to paired normal adjacent lung samples. FDR-corrected p< 0.001. (C) Expression values for DLC1 and CAV1 from data in B are positively correlated. (D-F) Director's challenge cohort, with more than 400 NSCLC, expression values for DLC1 and CAV1 are positively correlated (D), low expression of DLC1 predicts a poor prognosis (n=221) (E), and combining low CAV1 with low DLC1 does not further increase prognostic

significance compared with low DLC1 alone (F). The numbers indicate the number of patients in each group.